PSEM_2D: A physically based model of erosion processes at the plot scale

Guillaume Nord, Michel Esteves

PSEM_2D: A physically based model of erosion processes at the plot scale

Guillaume Nord and Michel Esteves

Laboratoire d'étude des Transferts en Hydrologie et Environnement (LTHE), UMR 5564, CNRS, INPG, IRD, UJF, Grenoble, France

Received 29 September 2004; revised 11 March 2005; accepted 16 May 2005; published 12 August 2005.

[1] This paper presents the development and first applications of the Plot Soil Erosion Model 2D (PSEM_2D). Infiltration is computed using a Green and Ampt model, overland flow is computed using the depth-averaged two-dimensional unsteady flow equations (Saint Venant equations), and soil erosion is computed by combining the equation of mass conservation of sediment and a detachment-transport coupling model for erosion by runoff. A shear stress approach is used to determine the transport capacity. The formation of a covering cohesionless layer as a result of depositing sediment and action of rainfall impact before runoff is considered. The erosion processes involved are rainfall and runoff detachment of original soil, rainfall redetachment, and overland flow entrainment of sediment from the deposited layer, and deposition. The model uses a single representative particle size. Complex rainfall events on natural slopes can be simulated. The accuracy of the predictions for erosion of planar surfaces is tested by comparison with observed data obtained from experiments and with an analytical solution. Good agreement between the calculated results and measured data was found. A sensitivity analysis was also performed. Limitations related to the description of overland flow on plane soil surface are pointed out. Finally, an application to a nonplanar natural surface of 75 m^2 illustrated the distribution of erosion and sedimentation over the plot.

Citation: Nord, G., and M. Esteves (2005), PSEM_2D: A physically based model of erosion processes at the plot scale, *Water Resour. Res.*, *41*, W08407, doi:10.1029/2004WR003690.

1. Introduction

[2] Erosion of topsoil by rain and runoff threatens food productivity and water quality. The intensification of productivity for the last 50 years has caused degradation of cropland topsoil. Soil erosion does not only affect crop productivity but also induces many off-site environmental impacts such as pollution of surface water associated with the transport of fine sediment.

[3] Because of the great range of types of soil and their physical properties erosion modeling has been rapidly necessary to estimate soil loss and to better understand erosion processes. Empirical models were developed using large body of data. The universal soil loss equation (USLE) presented by *Wischmeier and Smith* [1978] and then modified by *Renard et al.* [1994] has been historically the more widely used model of soil erosion at the field scale. However empirical models do not describe erosion processes and parameters involved are not directly measurable in situ. At the same time there has been an attempt to model rainfall erosion using physical principles. Early on, *Ellison* [1947] proposed to divide erosion into four subprocesses: detachment by raindrop impact, transport by rain splash, detachment by flow and transport by surface flow. This description of the processes has been widely used in erosion modeling. *Meyer and Wischmeier* [1969] introduced the ''rate-limiting'' concept meaning that sediment delivery is limited by either the detachment rate or the transport capacity of the flow depending on which has a lower value. *Foster and Meyer* [1972] used this concept and proposed a first-order detachment and transport coupling model for rill flow. The detachment rate is a linear function of the difference between the transport capacity and the actual sediment load. On the basis of the work of *Foster and Meyer* [1972] and *Foster* [1982], *Foster et al.* [1995] defined in WEPP the source term for erosion as the sum of a rill erosion rate and a delivery rate of sediment from interrill areas related to the detachment of sediment by rainfall impact. Other models such as KINEROS [*Woolhiser et al.*, 1990] and EUROSEM [*Morgan et al.*, 1998] use this explicit distinction between rill and interrill source term of sediment.

[4] *Hairsine and Rose* [1991] proposed another approach based on the concept of simultaneous erosion and deposition processes. Deposition is responsible for the formation of a cohesionless layer from which sediment can be removed again. [*Hairsine and Rose*, 1992a, 1992b] distinguished the detachment of previously uneroded soil due to rainfall impact and overland flow from the redetachment and reentrainment of sediment particles from the deposited layer. *Hairsine and Rose* [1992a] defined two common erosion situations referred to as rainfall driven erosion and flow driven erosion depending on whether the stream power exceeds a threshold value or not. Soil and eroded sediment are represented using a large number of size classes.

[5] A common shortcoming to these models of erosion is that the hillslope is represented by a planar land surface.

0043-1397/05/2004WR003690

However overland flow over a natural hillslope does not take the form of a film of uniform depth. Overland flow channelizes rapidly after a few meters and two types of regions appear. Interrill areas are extensive and characterized by very low flow depth, less than 1cm [*Hairsine and Rose*, 1991]. They are located between the rills and contribute therefore to flow into rills. Rills are small, ephemeral concentrated flow paths which function as both sediment source and sediment delivery systems for erosion on hillslopes. They are typically of the order of a centimeter, and slopes may be quite steep [*Nearing et al.*, 1997]. The spatial and temporal distribution of overland flow is of major importance to describe erosion at the plot and hillslope scale. However knowledge of these space-time dynamics remains poor. In the models mentioned above the morphological distinction between rill and interrill regions is rather theoretical. Rills and interrill areas are considered separately. Rills are represented by geometric parameters such as width and spacing of rills. The development of PSEM_2D is an attempt to improve the prediction of runoff hydraulics and soil erosion and model the interaction of hydraulic and sediment transport processes for non steady conditions in two dimensions. This model does not distinguish explicitly between rills and interrill areas. The same processes are involved all over the plot, which is typically of the order of 100 square meters. It is microtopography and hydraulic conditions that emphasize either the effects of rainfall or those of overland flow. As a first step before further development of the model a single representative particle size is used although the studies of *Sander et al.* [1996], *Hairsine et al.* [1999], *Heilig et al.* [2001], and *Beuselinck et al.* [2002] demonstrate clearly the need for multisize class depositional models. Here we present the model and its evaluation over a plane surface and an illustration of its capabilities to deal with a real topography plot.

2. Description of the Model

[6] PSEM_2D is a two-dimensional numerical model which is based on an explicit finite difference scheme coupling infiltration, overland flow and soil erosion processes for hillslopes. The model is designed to include nonconstant rainstorm with time evolution of rainfall rates.

2.1. Shallow Water Equations and Approximations

[7] Overland flow is described by the depth-averaged two-dimensional unsteady flow equations commonly referred to as the Saint Venant equations [*Zhang and Cundy*, 1989; *Esteves et al.*, 2000]:

$$\frac{\partial(uh)}{\partial x}+\frac{\partial(vh)}{\partial y}+\frac{\partial h}{\partial t}=R-I(x,y) \tag{1}$$

$$\frac{\partial u}{\partial t}+u\frac{\partial u}{\partial x}+v\frac{\partial u}{\partial y}+g\left[\frac{\partial h}{\partial x}+S_{fx}-S_{ox}\right]=0 \tag{2}$$

$$\frac{\partial v}{\partial t}+u\frac{\partial v}{\partial x}+v\frac{\partial v}{\partial y}+g\left[\frac{\partial h}{\partial y}+S_{fy}-S_{oy}\right]=0 \tag{3}$$

where h is the mean depth of flow, u and v the local depth-averaged velocities, R the rainfall intensity, I the rate of infiltration, g the gravitational constant. S_{ox} and S_{fx} and S_{oy} and S_{fy} are the ground slopes and the friction slopes in the x and y directions, respectively. The quantities appearing in all the equations are defined in the notation list.

[8] Equation (1) is the standard conservation of mass for water. Equations (2) and (3) are the momentum equations for the flow for each of the planar coordinate directions x and y. The friction slopes are approximated using the Darcy-Weisbach equations. Infiltration is computed using a Green and Ampt model. The model allows calculation of Hortonian overland flow and infiltration during complex events. More details about surface runoff processes, soil surface conditions and infiltration are given by *Esteves et al.* [2000].

2.2. Mass Conservation of Sediment

[9] The mathematical basis for modeling of non equilibrium sediment transport requires a mass balance equation for suspended sediment [*Bennet*, 1974; *Woolhiser et al.*, 1990]:

$$\frac{\partial(hc)}{\partial t}+\frac{\partial(uhc)}{\partial x}+\frac{\partial(vhc)}{\partial y}=\frac{\left(D_{rd\_d}+D_{rd\_rd}+D_{fd\_d}+D_{fd\_e}\right)}{\rho_s} \tag{4}$$

and a mass conservation for the deposited layer of loose sediment l_d expressed in its most general form as

$$\frac{\partial l_d}{\partial t}=-\frac{1}{\rho_s}\left(D_{rd\_rd}+D_{fd\_e}\right) \tag{5}$$

where c is the volumetric sediment concentration, ρ_s the sediment particle density, D_{rd_d} the detachment rate of sediment by rainfall from the soil, D_{rd_rd} the redetachment rate of sediment by rainfall from the deposited layer, D_{fd_d} the detachment/deposition rate of sediment from the soil by overland flow, D_{fd_e} the entrainment/deposition rate of sediment from the deposited layer by overland flow.

[10] This description implies that both the soil and the eroded fragments are represented by a median diameter. Sediment sorting associated with erosion processes is not possible. Moreover eroded sediment is transported as suspension only under the assumption that the velocity of sediment is the same as the flow velocity [*Bennet*, 1974].

2.3. Erosion Processes Represented in the Model

[11] Different processes of rainfall erosion are involved in the model. During a first phase where the shear stress of the flow τ_f is lower than the critical shear stress of the particle τ_c, we consider that rainfall has two major actions: disaggregation of the soil surface and local redistribution of sediment by splash. This phase includes the two modes of transport referred to by *Kinnell* [1999] as "raindrop detachment–splash transport" in the absence of runoff and "raindrop detachment–raindrop-induced flow transport" that occurs when the flow shear stress is insufficient to detach soil material and also insufficient to entrain loose sediment from the deposited layer. The model does not represent explicitly the transport of sediment by rain splash or raindrop-induced flow. We assume that the bed elevation does not change during this phase and that the sediment concentration in flow remains zero but breakdown of aggregates, raindrop impact, rain splash and subsequent

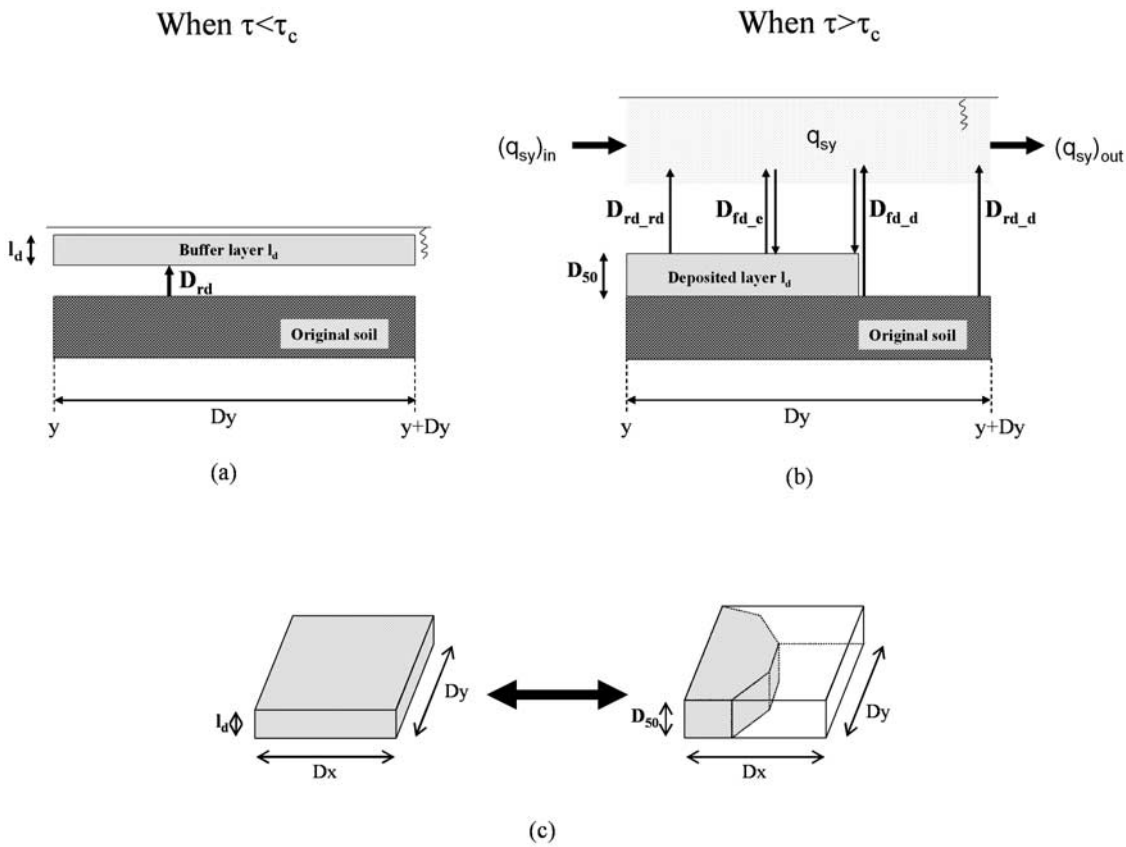

Figure 1. Erosion processes when the flow shear stress is (a) below the critical shear stress of the particle and (b) above the critical shear stress of the particle and (c) conceptualization of the layer of loose sediment. D_{rd} is the rate of disaggregation and redistribution of sediment by rain splash, D_{rd_d} is the sediment detachment rate from original soil by rainfall, D_{rd_rd} is the sediment redetachment rate from the deposited layer by rainfall, D_{fd_d} is the detachment/deposition rate of sediment from original soil by runoff, and D_{fd_e} is the entrainment/deposition rate of sediment from the deposited layer by runoff.

deposition contribute to fill up the buffer layer l_d with loose sediment as shown in Figure 1a. This layer has different strength characteristics compared to original soil. During this phase equation (4) does not apply but the equation of mass conservation of the deposited layer is required in a form slightly different from that proposed in equation (5):

$$\frac{\partial l_d}{\partial t} = \frac{1}{\rho_s}(D_{rd}) \tag{6}$$

where D_{rd} is the rate of aggregate breakdown and rainfall redistribution of sediment by splash.

[12] When the shear stress of the flow overcomes the critical shear stress of the particle, the flow has a transport capacity and is able to entrain sediment from the layer of loose sediment. This phase referred to as raindrop detachment–flow transport by *Kinnell* [1999] and "rain-flow transportation" by *Moss et al.* [1979] can explain an initial peak of sediment concentration if the previous mechanisms have produced a substantial layer of loose sediment. Therefore rainfall driven erosion which occurs when $\tau < \tau_c$ is not neglected but only delayed in the model. Once all the sediment from the buffer layer has been entrained a higher-flow shear stress is necessary to detach particles from original soil characterized by a critical shear stress τ_{soil} related to the soil shear strength [*Leonard and Richard*, 2004]. *Kinnell* [1999] names this process "flow detachment–flow transport." Figure 1b illustrates the processes involved during this phase. In these conditions equation (5) applies and the mass conservation equation for the deposited layer is expressed as in equation (6) for the net erosion case (D_{fd_d} and $D_{fd\_e} > 0$) or as follows for the deposition case (D_{fd_d} and $D_{fd\_e} < 0$):

$$\frac{\partial l_d}{\partial t} = -\frac{1}{\rho_s}\left(D_{rd\_rd} + D_{fd\_e} + D_{fd\_d}\right) \tag{7}$$

[13] A shortcoming to this overall description could come from the formulation of the shear stress acting on the bed. No component due to rainfall impact that would increase the turbulence of flow is taken into account as proposed by *Foster* [1982]. Only the flow shear stress is considered:

$$\tau_f = \sqrt{\left(\tau_{fx}^2 + \tau_{fy}^2\right)} \tag{8}$$

where

$$\tau_{fi} = g\rho_f h S_{fi} \tag{9}$$

Indice i indicates that variables are calculated in both directions x and y.

[14] Another point of discussion is the use of the critical shear stress of a spherical particle τ_c as a threshold for erosion mechanisms when a single representative particle size is used. The expression of τ_c is given by *Yang* [1996]:

$$\tau_c = \delta_s g\left(\rho_s - \rho_f\right) D_{50} \tag{10}$$

where δ_s is the critical dimensionless shear stress of the sediment set to 0.047 in this study as proposed by *Tayfur* [2002], ρ_f the water density, and D_{50} the median sediment particle diameter. The critical shear stress τ_c which rules the change between raindrop detachment–raindrop-induced flow transport and raindrop detachment–flow transport varies with size and density [*Kinnell*, 1999]. Therefore it is clear that different processes may occur at the same time depending on the type of particle considered. Using only a median diameter the model is not able to represent such a complexity. Further development will require representing soil and eroded fragments using a multisize class model. At this stage the use of a single representative particle size allows to study in more details the validity of the equations applied to describe the movement of particles over a natural hillslope.

2.4. Model of Soil Detachment by Rainfall

[15] The rainfall detachment and redetachment rates are determined using a model developed by *Li* [1979]:

Detachment
$$D_{rd\_d} = \alpha R^p \left(1 - \frac{h}{z_m}\right)(1 - \varepsilon) \tag{11}$$

Redetachment
$$D_{rd\_rd} = \alpha_d R^p \left(1 - \frac{h}{z_m}\right)\varepsilon \tag{12}$$

where

$$z_m = 3 \times \left(2.23 \times R^{0.182}\right) \tag{13}$$

z_m is the maximum penetration depth of raindrop splash. α is the rainfall erodibility for original soil and α_d is the rainfall erodibility for the deposited layer. *Proffitt et al.* [1991] and *Misra and Rose* [1995] showed that α_d was greater than α by approximately two orders of magnitude. The exponent p is set to 1.0 in this study according to the results of *Sharma et al.* [1993]. The third term on the right hand side of equations (11) and (12) represents the damping effect of rainfall with increasing flow depth. ε is conceptualized as the percentage of a grid cell covered by a deposited layer of depth the median particle diameter D_{50}. The volume of this layer is equal to the volume of a layer with a depth equal to the loose soil depth l_d which would be spread over the whole grid cell as shown in Figure 1c. Therefore ε is calculated as

$$\varepsilon = \frac{l_d}{D_{50}} \tag{14}$$

When $\varepsilon = 0$, it means the only processes involved are rainfall and flow detachment. On the other hand when $\varepsilon = 1$, there are only rainfall redetachment and flow entrainment.

[16] A similar model is used to express the rate of aggregate breakdown and rainfall redistribution of sediment by splash D_{rd} when the flow shear stress is lower than the critical shear stress τ_c:

$$D_{rd} = \alpha R^p \left(1 - \frac{h + l_d}{z_m}\right) \tag{15}$$

2.5. Model of Soil Detachment and Deposition by Runoff

[17] When sediment load is less than sediment transport capacity, the rates of runoff detachment and runoff entrainment are calculated using the model of *Foster et al.* [1995]:

Detachment
$$D_{fd\_d} = K_r\left(\tau_f - \tau_{soil}\right)\left(1 - \frac{q_s}{T_c}\right)(1 - \varepsilon) \tag{16}$$

Entrainment
$$D_{fd\_e} = K_r\left(\tau_f - \tau_c\right)\left(1 - \frac{q_s}{T_c}\right)\varepsilon \tag{17}$$

where K_r is the flow erodibility parameter, D_{fd_d} and D_{fd_e} are equal to zero when τ_f is inferior to τ_{soil} and τ_c respectively.

[18] When sediment load is greater than transport capacity, another expression is necessary to calculate the rates of deposition [*Foster et al.*, 1995]:

$$D_{fd\_d} = \frac{\varphi V_f}{q}(T_c - q_s)(1 - \varepsilon) \tag{18}$$

$$D_{fd\_e} = \frac{\varphi V_f}{q}(T_c - q_s)\varepsilon \tag{19}$$

where φ is a raindrop induced turbulence coefficient, V_f the particle settling velocity, and q the flow discharge per unit width in the flow direction. The value of the raindrop induced turbulence coefficient φ is assigned to 0.5 in this study [*Foster et al.*, 1995]. However recent research carried out by *Cochrane and Flanagan* [2001] showed that φ is rather comprised between 0.02 and 0.2. The role of this coefficient and more largely the mechanism of deposition are still not well understood. The particle settling velocity for the sediment V_f is derived from particle size and density, assuming the particles have drag characteristics and terminal fall velocities similar to those of spheres [*Woolhiser et al.*, 1990].

[19] It is questionable to use a discontinuous model for D_{fd_d} and D_{fd_e} depending on whether the sediment load is greater or lower than the transport capacity of flow. However the objective of this model is above all to test existing models of sediment transport over natural hillslopes. A version of the model based on the continuous process of deposition proposed by *Hairsine and Rose* [1991] is still under development and will be presented later.

2.6. Transport Capacity of the Flow

[20] Determination of the transport capacity is based on the shear stress of the flow [*Foster*, 1982]:

$$T_c = \eta\left(\tau_f - \tau_c\right)^k \tag{20}$$

where η is the coefficient of efficiency of sediment transport, and k an exponent.

[21] When τ_f is lower than τ_c, the transport capacity T_c is set to zero. The exponent k is taken as 1.5 in this study according to the study of *Finkner et al.* [1989].

3. Numerical Methods

3.1. Procedure of Resolution and Schemes

[22] The hydrological equations and erosion equations are solved independently within a time step since the sediment concentrations are usually small enough that they do not appreciably influence the mechanics of flow [*Bennet*, 1974]. Coupling of the erosion model to the numerical solutions of the Saint Venant equations is made by calculation of bed elevation at the end of each time step as a result of erosion or deposition. The numerical solution presented provides simulation of unsteady water and sediment movement under a rainfall event over a complex topography.

[23] The Saint Venant equations are solved at first using the MacCormack scheme [*MacCormak*, 1969], a second-order explicit finite difference scheme. The MacCormack scheme is a two step process providing second-order accuracy in both space and time without the need to calculate second-order time derivatives. The application of this scheme to the resolution of the Saint Venant equations is given by *Esteves et al.* [2000].

[24] The mass balance equation for sediment is solved at each time step after the resolution of the Saint Venant equations using a second-order centered explicit finite difference scheme. Concentration at $(t + \Delta t)$ is calculated using the values of h, u, v and c at time t:

$$\overline{c}_{i,j}^{t+dt} = c_{i,j}^{t} + \left(\frac{\partial c_{i,j}}{\partial t}\right)^{t} dt \tag{21}$$

where

$$\left(\frac{\partial c_{i,j}}{\partial t}\right)^{t} = \frac{1}{h_{i,j}^{t}} \left\{ \begin{array}{l} c_{i,j}^{t}\left[\left(\frac{\partial h_{i,j}}{\partial t}\right)_{av} + \frac{(q_x)_{i+1,j}^{t} - (q_x)_{i-1,j}^{t}}{2\Delta x} + \frac{\left(q_y\right)_{i,j+1}^{t} - \left(q_y\right)_{i,j-1}^{t}}{2\Delta y}\right] \\ -(q_x)_{i,j}^{t}\frac{c_{i+1,j}^{t} - c_{i-1,j}^{t}}{2\Delta x} - \left(q_y\right)_{i,j}^{t}\frac{c_{i,j+1}^{t} - c_{i,j-1}^{t}}{2\Delta y} \\ + \frac{(D_{rd\_d})_{i,j}^{t} + (D_{rd\_rd})_{i,j}^{t} + \left(D_{fd\_d}\right)_{i,j}^{t} + \left(D_{fd\_e}\right)_{i,j}^{t}}{\rho_s} \end{array} \right\} \tag{22}$$

Equation (22) is not implemented when the flow shear stress is lower than the critical shear stress of particle.

[25] Variation of the depth of the deposited layer is calculated at each time step using equations (5), (6) or (7). Topographic elevations are reestimated at the end of each time step to account for changes in geometric conditions due to erosion or deposition:

$$z_{i,j}^{t+dt} = z_{i,j}^{t} \tag{23}$$

$$z_{i,j}^{t+dt} = z_{i,j}^{t} - \frac{\left((D_{rd\_d})_{i,j}^{t} + (D_{rd\_rd})_{i,j}^{t} + \left(D_{fd\_d}\right)_{i,j}^{t} + \left(D_{fd\_e}\right)_{i,j}^{t}\right)}{\sqrt{1 - \left((S_{ox})_{i,j}^{t}\right)^2}\sqrt{1 - \left((S_{oy})_{i,j}^{t}\right)^2}} \frac{dt}{\rho_s} \tag{24}$$

The terms $\sqrt{1 - \left((S_{ox})_{i,j}^{t}\right)^2}$ and $\sqrt{1 - \left((S_{oy})_{i,j}^{t}\right)^2}$ mean that we use the projection of l_d on the z axis which is the axis perpendicular to the horizontal plane. Slopes in the x and y directions are recalculated after elevations accounting for the effects of changes in topography on hydrological and erosion variables.

3.2. Initial and Boundary Conditions

[26] In the laboratory applications presented herein, the shapes of the experimental plots are rectangles with three nonporous walls and an open boundary at the outlet. We used a uniform grid with two columns and one row (dummy cells) added to the physical plane to model wall boundary conditions (inward boundaries). *Esteves et al.* [2000] describe the benefits of the dummy cells for numerical purposes. The depths on the dummy cells are set equal to those of the adjacent inward boundaries. The flow velocities of the dummy cells are set to zero in the two directions. In the x direction the velocities are taken as zero along the both lateral boundaries of the physical domain [*Esteves et al.*, 2000]. The concentrations of the dummy cells are set equal to those of the cells located straight inward of the physical boundary. This condition means that no mass of sediment comes from outside the plot. No special condition is imposed to the lateral and upstream boundaries. Since depths and velocities at the outlet are not known, a special treatment for the outlet is required. Equations (1)–(4) are differentiated using forward differences. At that boundary no condition is required because the flow is supercritical.

[27] Experimental data against which the model was to be tested correspond to rain starting to fall on a dry soil surface. This straightforwardly translates in terms of numerical conditions into depths, velocities and concentrations all set equal to zero for each grid node. The model allows entering an initial value of l_d representing a layer of loose sediment existing before the simulated rainfall event, this layer being produced by a previous rainfall event.

4. Model Testing

4.1. Description of Experimental and Analytical Data

[28] In this section the performance of PSEM_2D is evaluated. Because of a lack of experimental data the model cannot be evaluated over non planar surfaces. For this reason we propose to test the model over planar surfaces using data from the literature. We use the experimental data of *Singer and Walker* [1983] and *Kilinc and Richardson*

Table 1. Predefined Parameters and Calibrated Parameters Obtained Using the Data of *Singer and Walker* [1983] and *Kilinc and Richardson* [1973][a]

Parameter	Value		Unit
	Singer and Walker	Kilinc and Richardson	
	Predefined Parameters		
D_{50}	2×10^{-5}	3.5×10^{-4}	m
ρ_s	2600	2600	kg m^{-3}
ρ_w	1000	1000	kg m^{-3}
ld_initial	0	0.2	m
p	1.0	1.0	
φ	0.5	0.5	
k	1.5	1.5	
	Calibrated Parameters		
Crust thickness	0	0	m
Soil water content deficit	0.2	0.2	
Saturated hydraulic conductivity[b]	3.25×10^{-6} 5.2×10^{-6}	2.1×10^{-7}	m s^{-1} m s^{-1}
Wetting front capillary pressure head	0.006	0.05	m
f	0.25	0.5	
α	0.0012	0.0015	kg m^{-2} mm^{-1}
α_d	0.012	0.015	kg m^{-2} mm^{-1}
Kr	0.005	0.024	s m^{-1}
τ_{soil}	0.15	0.3	Pa
η	0.04	0.023	m$^{0.5}$ s^2 kg$^{-0.5}$

[a]Singer and Walker data are from a test with 50 mm h^{-1} rainfall intensity, and Kilinc and Richardson data are from a test with 20% slope and 93 mm h^{-1} rainfall intensity.
[b]The saturated hydraulic conductivity is calibrated again for the test with 100 mm h^{-1} rainfall intensity.

[1973] and the analytical solution of *Govindaraju and Kavvas* [1991]. As an illustration we show the ability of PSEM_2D to run over non planar surfaces.

4.1.1. Experimental Data of *Singer and Walker* [1983]

[29] The experiment set up used by *Singer and Walker* [1983] was a laboratory flume (3.0 by 0.55 m) of 9% slope and a rainfall simulator. The soil was a fine sandy loam with a clay content of 13.9% and a high amount of silt plus very fine sand (59.2% in the range 2×10^{-6}–1×10^{-4} m). The median diameter D_{50} of the soil was 2×10^{-5} m. The final soil surface was smooth and hard to the touch. Details of the experimental conditions are given in the work of *Singer and Walker* [1983]. The major control variable was rainfall intensity. Bare soil surfaces were tested with two rainfall intensities (50 and 100 mm h^{-1}).

[30] Each event was allowed to run for 30 min. Measurements of flow depths under rainfall and runoff was difficult, but estimates made using small rods, driven vertically into the bed, indicated that for events with 50 mm h^{-1} rainfall, flow depths were 1×10^{-3}–2×10^{-3} m. No topographic data were measured but the authors mentioned that no major changes developed on the bed surface.

4.1.2. Experimental Data of *Kilinc and Richardson* [1973]

[31] *Kilinc and Richardson* [1973] performed rainfall simulations on a 1.52 m wide × 4.58 m long flume with an adjustable slope using commercial sprinklers on a 3 m risers, placed 3 m apart along the sides of the flume. The flume was filled with compacted sandy soil composed of 90% sand and 10% silt and clay. The soil had a nonuniform size distribution with a median diameter of 3.5×10^{-4} m. The soil surface was leveled and smoothed before each run. The major controlled variables were rainfall intensity and soil surface slope. Infiltration and erodibility of surface were supposed constant.

[32] Slopes ranging from 5.7 to 40% were tested with four rainfall intensities (32, 57, 93, and 117 mm h^{-1}). Each run was 1 hour long. The details of the experiments can be obtained from the work of *Kilinc and Richardson* [1973].

[33] In terms of flow depth and microtopography no data were collected. The authors reported that measurements taken by the point gauge with the idea of measuring depth of flow at different sections of the land surface during rainfall proved unreliable, partly because of rainfall impact depressions and partly because of the movable bed.

4.1.3. Analytical Solution of *Govindaraju and Kavvas* [1991]

[34] *Govindaraju et al.* [1990] developed a physically based hydrologic model for surface overland flow which provides analytical solutions for temporal variations in rainfall and infiltration. Later *Govindaraju and Kavvas* [1991] coupled this model to the erosion model of *Foster and Meyer* [1972] and developed an analytical solution for the time space varying sediment discharges over steep planar hillslopes.

4.2. Description of Input Parameters Needed to Run the Model

[35] Only bare soil surfaces are represented at this stage of development. No direct vegetation effects (interception, roughness) are taken into account. The Darcy-Weisbach friction factor *f* assumed constant over the rainfall event can be entered as a distributed parameter. The ground slopes in the *x* and *y* directions (S_{ox} and S_{oy}) have to be provided.

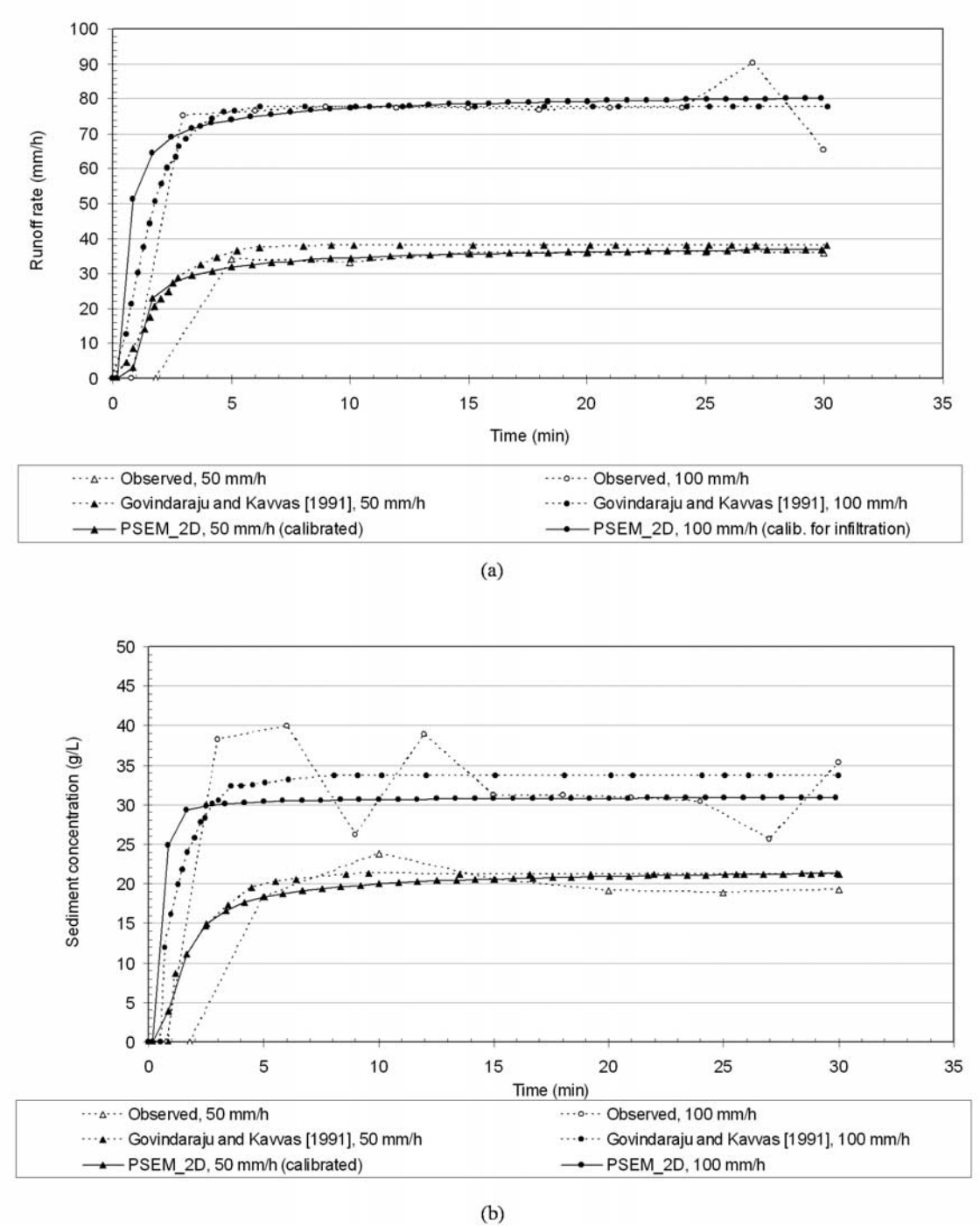

Figure 2. Comparison of (a) numerical outflow discharge hydrographs and (b) numerical sedimentographs obtained using PSEM_2D with the results of *Govindaraju and Kavvas* [1991] and the experimentally observed results of *Singer and Walker* [1983].

Infiltration parameters needed to run the model are the wetting front capillary pressure head, the saturated hydraulic conductivity, and the water content deficit of the soil. The model is also able to account for a crust at the surface of the soil. In this case the thickness and the saturated hydraulic conductivity of the crust are needed. These input parameters are required for each type of soil as well as a map of spatial distribution of the soil types.

[36] To calculate soil erosion some parameters are needed as single values: the density of water ρ_f and sediment ρ_s, the median particle diameter of sediment D_{50}, the coefficient of efficiency of sediment transport η, the critical shear stress of the soil τ_{soil}, and the initial depth of the deposited layer $l_{d\_initial}$. The other parameters that can be entered as spatial distribution are the flow erodibility parameter K_r, the rainfall erodibility coefficient for original soil α, the rainfall

erodibility coefficient for the deposited layer α_d, and the elevation of the soil surface z.

[37] The results presented here do not address the effect of spatial variability of rainfall and soil characteristics. The model is restricted to the case where soil and roughness are homogeneous within the physical domain.

4.3. Comparison of the Model With Observed Data Collected by *Singer and Walker* [1983]

[38] We first compare the performance of the model with results obtained from experiments conducted by *Singer and Walker* [1983]. The soil surface is represented as a plane element of 3.0 m long by 0.55 m wide using uniform grid cells of 0.05 m by 0.05 m.

[39] Calibration is carried out manually using a test with 50 mm h^{-1} rainfall intensity. The first step consists of calibrating the Darcy-Weisbach friction factor and the infiltration parameters, infiltration being computed using the Green and Ampt model. The erosion parameters are then determined. Some of them have been defined in the previous sections and others are calibrated as listed in Table 1. The rainfall erodibility parameters derived by *Sharma et al.* [1993] vary from 0.00012 to 0.015 kg m^{-2} mm^{-1}. We decide arbitrarily to give at α_d a value 10 times greater than α following the observations of *Proffitt et al.* [1991]. According to *Foster et al.* [1995], Kr ranges between 1×10^{-5} and 4×10^{-3} s m^{-1} for rangeland soil and between 0.002 and 0.05 s m^{-1} for cropland soil. In this study the soil can be considered as an agricultural soil since it was disturbed when filling the flume. The value of τ_{soil} is estimated using the WEPP soil database [*Foster et al.*, 1995]. In the work of *Finkner et al.* [1989], η varies between about 0.01 and 0.045 $m^{0.5}$ s^2 $kg^{-0.5}$. The calibrated parameters are then employed to evaluate the model under 100 mm h^{-1} rainfall intensity. An important point is that the calibrated parameters overestimated the water discharge for 100 mm h^{-1} rainfall intensity. We obtained a numerical water discharge of 87 mm h^{-1} instead of the averaged 78 mm h^{-1} measured at steady state. Since the main purpose of this study was to address the effect of rainfall intensity variation on sediment concentration under a given parameterization of erosion it was decided to evaluate again the saturated hydraulic conductivity. We found a value of 5.2 mm h^{-1}. Figure 2 shows the comparison of numerical outflow discharge hydrographs (Figure 2a) and numerical sedimentographs (Figure 2b) obtained using PSEM_2D with the analytical results of *Govindaraju and Kavvas* [1991] and the experimentally observed results of *Singer and Walker* [1983].

[40] These results show that PSEM_2D is capable of reproducing observed values quite well. The agreement between PSEM_2D and the results of *Govindaraju and Kavvas* [1991] is reasonably good. The maximum flow depth calculated at the end of the plane is 3×10^{-4} m whereas the estimates made by *Singer and Walker* [1983] were between 1×10^{-3}–2×10^{-3} m. The model can reproduce good hydrographs as shown in Figure 2a but underestimates flow depths. The model reproduces the increase of sediment load with the increase of rainfall intensity as shown in Figure 2b. The model underestimates the 100 mm h^{-1} test during the first 5 minutes. Larger rainfall erodibility could contribute to the formation of a larger buffer layer before runoff and an initial peak of sediment concentration. Another point that can explain the discrepancies between the results at steady state is the determination of flow detachment capacity and sediment transport capacity since the model also shows that the contribution of runoff detachment to the sediment yield is predominant under this parameterization compared to the other processes.

4.4. Comparison of the Model With Observed Data Collected by *Kilinc and Richardson* [1973]

[41] In this section we examine the response of the model to changes in both rainfall intensity and slope steepness, two factors affecting very much erosion processes. We use the observed values of *Kilinc and Richardson* [1973]. Grid cells are 0.05 m by 0.05 m. The comparison is limited to the cases of 15, 20, and 30% slopes with rainfall intensity of 93 mm h^{-1} and 117 mm h^{-1}. The selected runs correspond to the runs chosen by *Govindaraju and Kavvas* [1991] to validate their analytical solution for modeling erosion processes over steep slopes. A calibration is first carried out as described previously using the case of 20% slope with 93 mm h^{-1} rainfall intensity. The data available to calibrate the model include the averaged water discharge at steady state and the continuous sediment discharge at the end of the flume. Because of the lack of topographic data the soil surface is represented as a plane. The values of the parameters are listed in Table 1. The water discharge calculated at the outlet after 60 min of simulation using these parameters is 1.144×10^{-4} m^2 s^{-1}, about 6% inferior to the averaged value measured at steady state.

[42] The sediment discharge observed at the outlet is high. Its value at steady state is 0.022 kg m^{-1} s^{-1} with a sediment concentration of 154.2 g L^{-1}. To reproduce this level of erosion the soil has to be considered as a non cohesive material which is not irrelevant as the D_{50} is in the range of medium sand and the soil has been disturbed during filling up of the flume. Therefore $l_{d\_initial}$ is set to 0.2 m representing the thickness of the soil bed. The only processes involved are therefore redetachment by rainfall and flow entrainment. The value of the critical shear stress of the soil is useless in this case.

[43] The calibrated parameters are then applied to the cases of 15 and 30% slopes with 93 and 117 mm h^{-1} rainfall intensity and the case of 20% slope with 117 mm h^{-1} rainfall intensity. Using the calibrated parameters for infiltration, the numerical water discharges at steady state at the end of the plane are all inferior of about 5 to 9% to the observed values. Figure 3 shows the comparison of the numerical sediment discharges at the outlet of the flume using PSEM_2D with the observed data of *Kilinc and Richardson* [1973] and the results of *Govindaraju and Kavvas* [1991].

[44] The model reproduces quite well the variations in sediment discharge related to the changes in slope steepness and rainfall intensity. The model does the best for the case of 30% slope and 93 mm h^{-1} rainfall intensity. Numerical results overestimate observed data under 93 mm.h^{-1} and 117 mm h^{-1} rainfall intensities for the case of 15% slope. On the other hand the model underestimates experimental results under 117 mm h^{-1} rainfall intensity for the cases of 20% of 30% slope. The discrepancies between numerical results and observed data may be partly due to the lack of data available to calibrate the hydrological parameters.

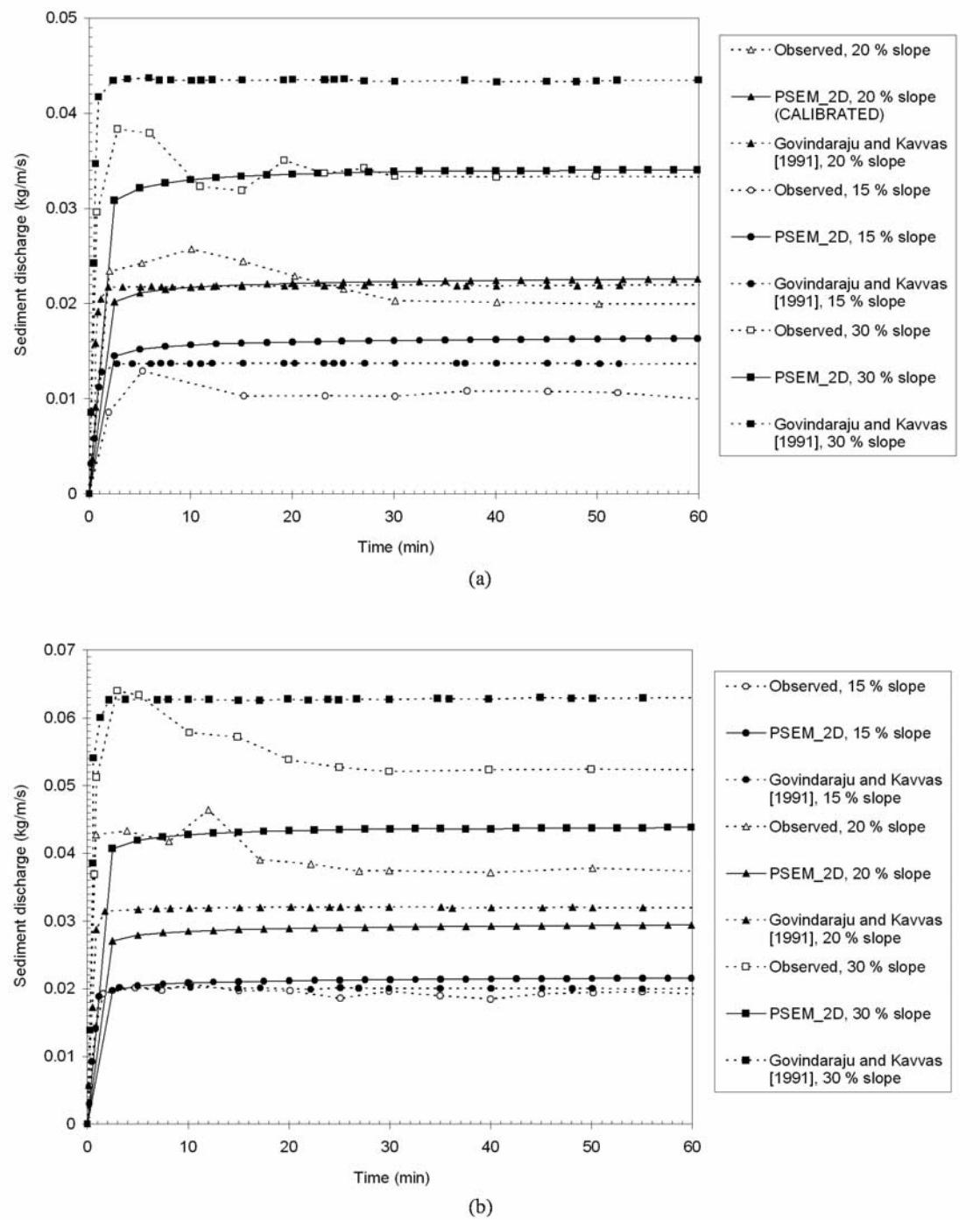

Figure 3. Comparison of the numerical sediment discharges obtained using PSEM_2D with the experimentally observed results of *Kilinc and Richardson* [1973] and the analytical results of *Govindaraju and Kavvas* [1991]. (a) Rainfall intensity of 93 mm h^{-1}. Slopes are 15, 20, and 30%. (b) Rainfall intensity of 117 mm h^{-1}. Slopes are 15, 20, and 30%.

Considering the high sediment discharges observed especially for steep slopes one can suppose that the flow concentrated into rills instead of remaining as a uniform sheet flow. Concentration of the flow into rills could have led to higher-flow depths and greater shear stresses than what gives uniform sheet flow. Therefore calibrated erosion parameters can have been overestimated in order to compensate for the low shear stress of flow. This compensation may turn out to be insufficient when rainfall intensity and then water discharge increase on steep slopes (20 and 30%). On the over hand the compensation may appear excessive on low slope (15%) even when rainfall intensity increases. It is possible that for the case of 15% slope overland flow did not concentrate into rills.

Table 2. Ranges of Variation of the Parameters Tested in the Sensitivity Analysis

Symbol	Description	Range	Unit
D_{50}	median particle diameter	1×10^{-6}–5×10^{-4}	m
ld_initial	loose soil depth at the beginning of the simulation	0–0.01	m
α	rainfall erodibility parameter for original soil	1.2×10^{-4}–1.5×10^{-2}	kg m^{-2} mm^{-1}
Kr	flow erodibility parameter	1×10^{-5}–5×10^{-2}	s m^{-1}
τ_{soil}	critical shear stress of original soil	0.05–0.3	Pa
η	coefficient of efficiency of sediment transport	0.01–0.05	m$^{0.5}$ kg$^{-0.5}$ s^2
δ_s	critical dimensionless shear stress	0–0.1	
f	Darcy-Weisbach friction factor	0.25–1.0	

4.5. Sensitivity Analysis

[45] A sensitivity analysis was carried out to determine how the variations of the parameters affect the mass sediment concentration at the outlet of the plot (C in g L^{-1}). We focus on the set of parameters calibrated with the data of *Singer and Walker* [1983] and listed in Table 1. The ranges of variations of these parameters are given in Table 2. Slope is 9% and rainfall intensity is 50 mm h^{-1}. The sensitivity analysis consists of changing the value of one single parameter at a time and remaining the others constant. We compare the values of the sediment concentration with the reference value obtained using the set of calibrated parameters. The steady state is obtained after 35 min of simulation. Therefore rainfall is applied during 35 min instead of the 30 min simulation in the experiment of *Singer and Walker* [1983]. The effects of the variations of α_d are not tested. When $l_{d\_initial} = 0.010$ m is entered rainfall redetachment and flow entrainment are involved instead of rainfall detachment and flow detachment of the reference case. φ is not tested since there is no deposition in the conditions tested. All the results are plotted in Figure 4.

[46] The most sensitive parameters are τ_{soil}, K_r, and f. All these parameters are related to runoff erosion which is the dominant process in these conditions. τ_{soil} is a threshold value of shear stress under which no detachment by flow takes place. The greater K_r, the closer to the maximum value defined by the transport capacity the sediment concentration is. f is a factor accounting for roughness. When f rises the flow depth rises too leading to an increase of the flow shear stress and the flow detachment rate. When f is high, velocity is lower and rill erosion should be less important. The model does not reproduce this decrease of rill erosion with roughness since there is no partitioning of the shear stress into grain shear stress and form shear stress. τ_{soil} is the most sensitive parameter tested. A decrease of 33% of τ_{soil} leads to an increase of C of 100%. On the other hand an increase of τ_{soil} of about 100% stops the detachment of sediment by the flow and brings the sediment concentration rapidly close to zero. K_r and f are just a little bit less sensitive. An increase of 100% of both K_r and f makes rise C of about 75%.

[47] The parameter related to rainfall erosion α is less efficient to change the value of C. An increase of 500% of α leads to an increase of less than 40% of C. Variations of C with α are linear since the detachment rate is a linear function of α and R as expressed in equations (11) and (12).

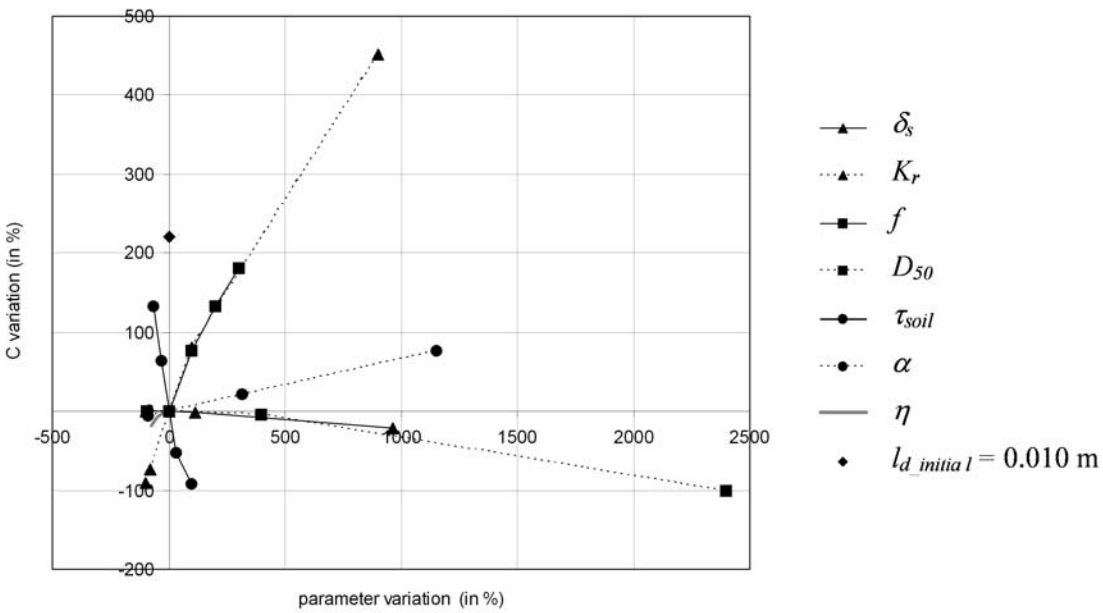

Figure 4. Variations in percentage of the mass sediment concentration at the outlet of the plot when steady state is reached versus variations in percentage of each tested parameter, all the other parameters keeping the calibrated value giving in Table 1.

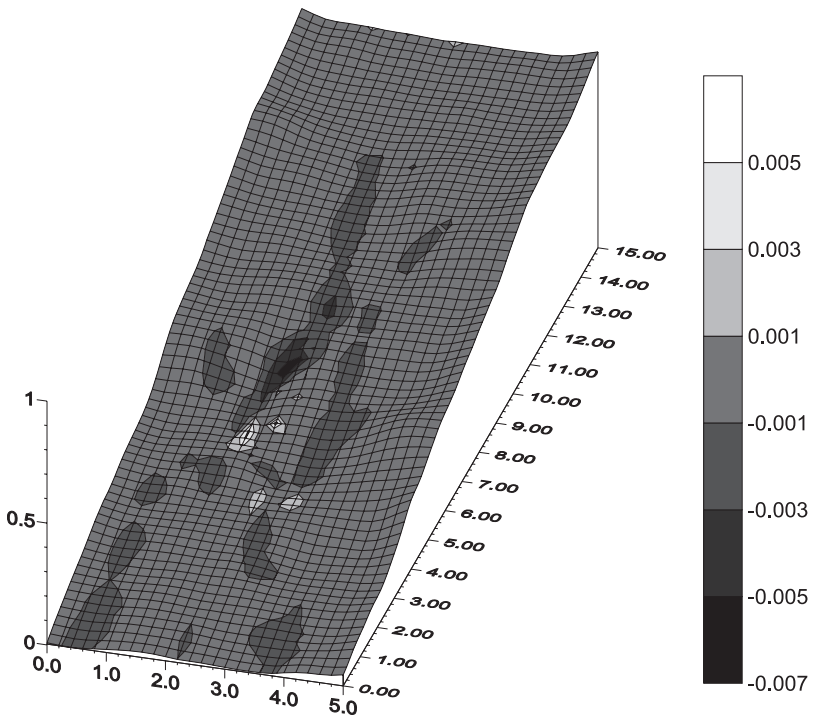

Figure 5. Computed variations of the soil surface elevations in meters at the end of the simulation (the lines are the boundaries between the regions of net erosion and net deposition).

[48] The η and δ_s parameters are not very sensitive. The major effect of the variation of η is a decrease of C of less than 20%. Furthermore the range of variation of η is quite tight. Outside this range the value of the sediment transport capacity is not relevant. Concerning δ_s an increase of 400% makes diminish C of 5%.

[49] In the conditions tested here D_{50} is not very sensitive. The main reason is that the model does not simulate deposition over this plane element whereas deposition is a highly selective process. The only selectivity that remains is related to the process of entrainment by runoff. C takes the value zero when the critical shear stress of the particle overcomes the shear stress of the flow at the outlet.

[50] One can see that entering a value different of zero for $l_{d\_initial}$ produces a sediment concentration more than 200% greater than the reference concentration. This shows the efficiency of the rainfall redetachment and flow entrainment processes.

4.6. Illustration of the Use of PSEM_2D Over a Nonplanar Surface

[51] To illustrate the capacity of PSEM_2D to run over natural surfaces the model is applied to the plot used by *Esteves et al.* [2000]. The plot is 15 m long by 5 m wide. A detailed topographic survey was made using a 0.2 m by 0.2 m grid. Average slopes are 0.0196 and 0.064 in the x and y directions. No validation is possible since no measured data of sediment are available. As an example the model is run using the parameters obtained after calibration from the data of *Singer and Walker* [1983] for the case of 50 mm.h^{-1} rainfall intensity (Table 1). The median diameter is 2×10^{-5} m and the corresponding effective fall velocity given by the model is 2.57×10^{-4} m s^{-1}. The interactions of hydraulic and sediment transport processes over a natural surface under a natural complex rainfall event are tested. The simulation lasted for 135 min. The results show that the model is capable to deal with complex rainfall events and natural slopes.

[52] Figure 5 is a map of net erosion. It is calculated as the difference between soil surface elevation at the end of the simulation and before the rainfall event. Negative values correspond to zones of net erosion and positive values to zones of net deposition. The highest values of erosion are located in a zone of steep slopes and concentrated overland flow as seen in Figure 6. Deposition occurs in concave zones where slope steepness reduces rapidly. The maximum values of deposition are located just downstream the highest values of erosion. The thickness of the deposited layer is about 0.004 m. It is sufficient to divert runoff as shown in Figure 6. One can see that runoff flows in a main rill located on the right hand side of the plot, upstream the outlet, at the beginning of the simulation. On the other hand, runoff flows in two separated rills near the end of the simulation. Therefore the model can handle changes of microtopography due to erosion. This example shows that the model is capable of reproducing partly the dynamics of hydrological and erosion processes on natural surfaces.

5. Conclusion

[53] The development of a physically based model for overland flow and erosion at the plot scale has been described. This model can be applied to natural slopes and complex rainfall events at the plot scale. The model includes a specific description of the role of cohesion and the formulation of a layer of loose sediment. It divides the erosive action of rainfall and overland flow between eroding original soil and reintroducing sediment from the layer of

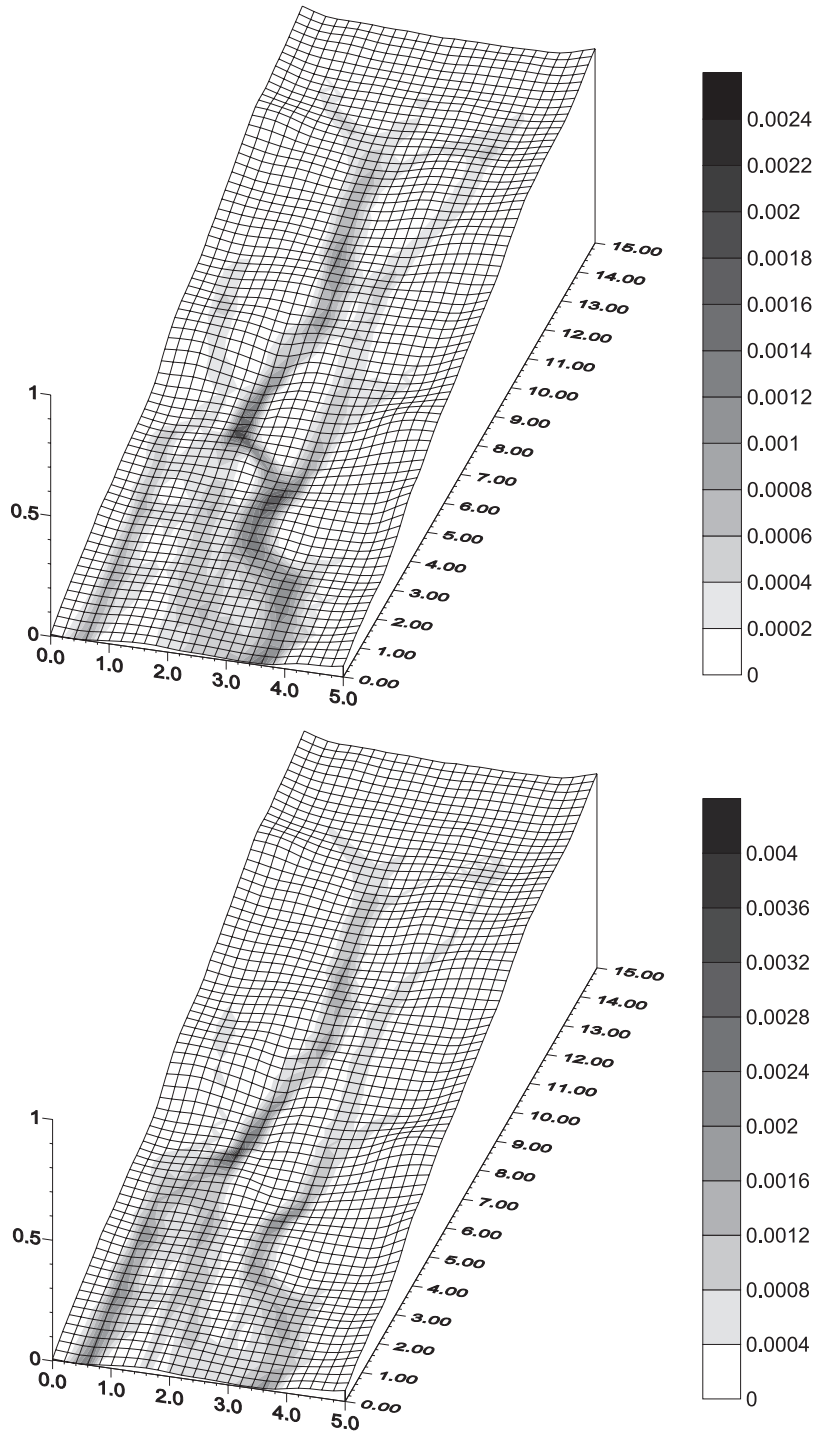

Figure 6. (top) Computed flow depths at the beginning of the simulation. (bottom) Computed flow depths close to the end of the hydrograph. The dimension for the flow depths is in meters.

loose sediment. The model uses a single-class particle size. A numerical two-dimensional model combining the shallow water equations and the Green and Ampt equation had been developed by *Esteves et al.* [2000] to reproduce overland flow production and transfer. The numerical scheme has been completed to incorporate calculation of erosion. The purpose of such modeling is to get a better understanding of the effects of microtopography on the distribution of overland flow and the interactions between hydrological and erosion processes. No data were available to validate the model on natural slopes. The performance of the model was thus tested on plane soil surfaces by comparing the numerical results with the observed data of *Singer and Walker* [1983] and *Kilinc and Richardson* [1973] and the analytical results of *Govindaraju and Kavvas* [1991] on the basis of calibrated hydrological and erosion parameters. Good agreement was found between the numerical results and the measured data. It was emphasized that a good descrip-

tion of the hydrological processes is necessary to well calibrate the erosion parameters. This description should consider the distribution of overland flow over the soil surface.

[54] Although an illustration of the capability of the model to run over non planar surfaces was presented emphasizing the complex relationship existing between overland flow and soil erosion, there is still a need to evaluate the model over natural soil surfaces.

Notation

c mass sediment concentration, $m^3\ m^{-3}$.
C volume sediment concentration, $g\ L^{-1}$.
D_{rd} rate of disaggregation and redistribution of sediment by rain splash, $kg\ m^{-2}\ s^{-1}$.
D_{rd_d} sediment detachment rate from original soil by rainfall, $kg\ m^{-2}\ s^{-1}$.
D_{rd_rd} sediment redetachment rate from the deposited layer by rainfall, $kg\ m^{-2}\ s^{-1}$.
D_{fd_d} detachment/deposition rate of sediment from original soil by runoff, $kg\ m^{-2}\ s^{-1}$.
D_{fd_e} entrainment/deposition rate of sediment from the deposited layer by runoff, $kg\ m^{-2}\ s^{-1}$.
D_{50} median sediment particle diameter, m.
f Darcy-Weisbach friction factor.
g gravitational acceleration, $m\ s^{-2}$.
h flow depth, m.
I rate of infiltration, $m\ s^{-1}$.
k exponent taken as 1.5 in this study.
K_r flow erodibility parameter, $s\ m^{-1}$.
l_d loose soil depth, m.
$l_{d\_initial}$ loose soil depth at the beginning of the simulation, m.
p an exponent taken as 1.0 in this study.
q flow discharge per unit width in the flow direction, $m^3\ s^{-1}\ m^{-1}$.
q_s sediment discharge per unit flow width in the flow direction, $kg\ m^{-1}\ s^{-1}$.
R rainfall intensity, $m\ s^{-1}$.
S_o ground slope.
S_f friction slope.
T_c sediment transport capacity of the flow, $kg\ m^{-1}\ s^{-1}$.
u flow velocity in the x direction, $m\ s^{-1}$.
v flow velocity in the y direction, $m\ s^{-1}$.
V_f effective fall velocity, $m\ s^{-1}$.
z topographic elevation of the soil surface, m.
z_m maximum penetration depth of raindrop splash, m.
α rainfall erodibility parameter for original soil, $kg\ m^{-2}\ mm^{-1}$.
α_d rainfall erodibility parameter for the deposited layer, $kg\ m^{-2}\ mm^{-1}$.
δ_s critical dimensionless shear stress.
ε percentage of a grid cell covered by a deposited layer of depth D_{50}.
η coefficient of efficiency of sediment transport, $m^{0.5}\ s^2\ kg^{-0.5}$.
φ raindrop induced turbulence coefficient taken as 0.5 in this study.
ρ_f water density, $kg\ m^{-3}$.
ρ_s sediment particle density, $kg\ m^{-3}$.
τ_f flow shear stress in the flow direction, Pa.
τ_c critical shear stress of a spherical sediment particle, Pa.
τ_{soil} critical shear stress of original soil, Pa.

[55] **Acknowledgments.** The authors are grateful for the financial support provided by IRD (Institut de Recherche pour le Développement) and the French National Research Program on Hydrology (PNRH). The authors thank the two anonymous reviewers for providing very helpful comments that have improved the clarity and quality of this paper.

References

Bennet, J. P. (1974), Concepts of mathematical modeling of sediment yield, *Water Resour. Res.*, *10*(3), 485–492.

Beuselinck, L., P.-B. Hairsine, G. Govers, and J. Poesen (2002), Evaluating a single-class net deposition equation in overland flow conditions, *Water Resour. Res.*, *38*(7), 1110, doi:10.1029/2001WR000248.

Cochrane, T. A., and D. C. Flanagan (2001), Deposition processes in a simulated rill, in *Soil Erosion Research for the 21st Century*, edited by J. C. Ascough II and D. C. Flanagan, pp. 139–142, Am. Soc. of Agric. Eng., St. Joseph, Mich.

Ellison, W. D. (1947), Soil erosion studies—Part I, *Agric. Eng.*, *28*, 145–146.

Esteves, M., X. Faucher, S. Galle, and M. Vauclin (2000), Overland flow and infiltration modelling for small plots during unsteady rain: Numerical results versus observed values, *J. Hydrol.*, *228*(3), 265–282.

Finkner, S. C., M. A. Nearing, G. R. Foster, and J. E. Gilley (1989), A simplified equation for modeling sediment transport capacity, *Trans. ASAE*, *32*(5), 1545–1550.

Foster, G. R. (1982), Modeling the erosion process, in *Hydrologic Modeling of Small Watersheds*, *ASAE Monogr. Ser.*, vol. 5, edited by C. T. Haan and D. L. Brakensiek, pp. 295–380, Am. Soc. of Agric. Eng., St. Joseph, Mich.

Foster, G. R., and L. D. Meyer (1972), A closed-form soil erosion equation for upland areas, in *Sedimentation Symposium to Honor Prof. H. A. Einstein*, edited by H. W. Shen, pp. 12.11–12.19, Colo. State Univ., Fort Collins.

Foster, G. R., D. C. Flanagan, M. A. Nearing, L. J. Lane, L. M. Risse, and S. C. Finkner (1995), Hillslope erosion component, in *Water Erosion Prediction Project: Hillslope Profile and Watershed Model Documentation*, edited by D. C. Flanagan and M. A. Nearing, *USDA NSERL Rep. 10*, chap. 11, pp. 11.1–11.12, Natl. Soil Erosion Res. Lab., Agric. Res. Serv., U.S. Dep. of Agric., West Lafayette, Indiana.

Govindaraju, R. S., and M. L. Kavvas (1991), Modeling the erosion process over steep slopes: Approximate analytical solutions, *J. Hydrol.*, *127*(1–4), 279–305.

Govindaraju, R. S., M. L. Kavvas, and S. E. Jones (1990), Approximate analytical solutions for overland flows, *Water Resour. Res.*, *26*(12), 2903–2912.

Hairsine, P. B., and C. W. Rose (1991), Rainfall detachment and deposition: Sediment transport in the absence of flow-driven processes, *Soil Sci. Soc. Am. J.*, *55*(2), 320–324.

Hairsine, P.-B., and C.-W. Rose (1992a), Modeling water erosion due to overland flow using physical principles: 1. Sheet flow, *Water Resour. Res.*, *28*(1), 237–243.

Hairsine, P.-B., and C.-W. Rose (1992b), Modeling water erosion due to overland flow using physical principles: 2. Rill flow, *Water Resour. Res.*, *28*(1), 245–250.

Hairsine, P. B., G. C. Sander, C. W. Rose, J.-Y. Parlange, W. L. Hogarth, I. Lisle, and H. Rouhipour (1999), Unsteady soil erosion due to rainfall impact: A model of sediment sorting on the hillslope, *J. Hydrol.*, *220*(3–4), 115–128.

Heilig, A., D. DeBruyn, M. Walter, C. Rose, J. Parlange, T. Steenhuis, G. Sander, P. Hairsine, W. Hogarth, and L. Walker (2001), Testing a mechanistic soil erosion model with a simple experiment, *J. Hydrol.*, *244*(1–2), 9–16.

Kilinc, M., and E. V. Richardson (1973), Mechanics of soil erosion from overland flow generated by simulated rainfall, *Hydrol. Pap. 63*, 54 pp., Colo. State Univ., Fort Collins.

Kinnell, P. I. A. (1999), Discussion on "The European Soil Erosion Model (EUROSEM): A dynamic approach for predicting sediment transport from fields and small catchments", *Earth Surf. Processes Landforms*, *24*, 563–565.

Leonard, J., and G. Richard (2004), Estimation of runoff critical shear stress for soil erosion from soil shear strength, *Catena*, *57*, 233–249.

Li, R. M. (1979), Water and sediment routing from watersheds, in *Modeling of rivers*, edited by H. W. Shen, John Wiley, Hoboken, N. J.

MacCormak, R. W. (1969), The effect of viscosity in hypervelocity impact cratering, *Pap. 69-354*, Am. Inst. Aeronaut. Astronaut., Reston, Va.

Meyer, L. D., and W. H. Wischmeier (1969), Mathematical simulation of the process of soil erosion by water, *Trans. ASAE*, *12*(6), 754–762.

Misra, R. K., and C. W. Rose (1995), An examination of the relationship between erodibility parameters and soil strength, *Aust. J. Soil Res.*, *33*, 715–732.

Morgan, R. P. C., J. N. Quinton, R. E. Smith, G. Govers, J. W. A. Poesen, K. Auerswald, G. Chisci, D. Torri, and M. E. Styczen (1998), The European Soil Erosion Model (EUROSEM): A dynamic approach for predicting sediment transport from fields and small catchments, *Earth Surf. Processes Landforms*, *23*(6), 527–544.

Moss, A. J., L. Walker, and J. Hutka (1979), Raindrop-stimulated transportation in shallow water flows: An experimental study, *Sediment. Geol.*, *22*, 165–184.

Nearing, M. A., L. D. Norton, D. A. Bulgakov, G. A. Larionov, L. T. West, and K. M. Dontsova (1997), Hydraulics and erosion in eroding rills, *Water Resour. Res.*, *33*(4), 865–876.

Proffitt, A. P. B., C. W. Rose, and P. B. Hairsine (1991), Rainfall detachment and deposition: Experiments with low slopes and significant water depths, *Soil Sci. Soc. Am. J.*, *55*(2), 325–332.

Renard, K. G., J. M. Laflen, G. R. Foster, and D. K. MacCool (1994), The revised universal soil loss equation, in *Soil Erosion Research Methods*, edited by R. Lal, pp. 105–124, Soil and Water Conserv. Soc., Ankeny, Iowa.

Sander, G. C., P. B. Hairsine, C. W. Rose, D. Cassidy, J.-Y. Parlange, W. L. Hogarth, and I. G. Lisle (1996), Unsteady soil erosion model, analytical solutions and comparison with experimental results, *J. Hydrol.*, *178*(1–4), 351–367.

Sharma, P. P., S. C. Gupta, and G. R. Foster (1993), Predicting soil detachment by raindrops, *Soil Sci. Soc. Am. J.*, *57*(3), 674–680.

Singer, M. J., and P. H. Walker (1983), Rainfall-runoff in soil erosion with simulated rainfall, overland flow and cover, *Aust. J. Soil Res.*, *21*, 109–122.

Tayfur, G. (2002), Applicability of sediment transport capacity models for nonsteady state erosion from steep slopes, *J. Hydrol. Eng.*, *7*(3), 252–259.

Wischmeier, W. H., and D. D. Smith (1978), Predicting rainfall-erosion losses—A guide to conservation planning, *Agric. Handbk. 537*, U.S. Dep. of Agric., Washington, D. C.

Woolhiser, D. A., R. E. Smith, and D. C. Goodrich (1990), KINEROS, A kinematic runoff and erosion model: Documentation and user manual, *Rep. ASR-77*, 130 pp., Agric. Res. Serv., U.S. Dep. of. Agric., Washington, D. C.

Yang, C. T. (1996), *Sediment Transport: Theory and Practice*, 396 pp., McGraw-Hill, New York.

Zhang, W., and T. W. Cundy (1989), Modeling of two dimensional overland flow, *Water Resour. Res.*, *25*, 2019–2035.

M. Esteves and G. Nord, Laboratoire d'étude des Transferts en Hydrologie et Environnement (LTHE), UMR 5564, CNRS, INPG, IRD, UJF, BP 53, F-38041 Grenoble Cedex 9, France. (guillaume.nord@hmg.inpg.fr)